Developmental Biology **237,** 130–144 (2001)
doi:10.1006/dbio.2001.0365, available online at http://www.idealibrary.com on IDEAL®

Hoxb2 and Hoxb4 Act Together to Specify Ventral Body Wall Formation

Nancy R. Manley,*,[1] Jeffery R. Barrow,† Tianshu Zhang,† and Mario R. Capecchi†

**Institute of Molecular Medicine and Genetics, Department of Pediatrics, Medical College of Georgia, Augusta, Georgia 30912; and †Howard Hughes Medical Institute, Department of Human Genetics, University of Utah School of Medicine, Salt Lake City, Utah 84112-5331*

Three different alleles of the *Hoxb4* locus were generated by gene targeting in mice. Two alleles contain insertions of a selectable marker in the first exon in either orientation, and, in the third, the selectable marker was removed, resulting in premature termination of the protein. Presence and orientation of the selectable marker correlated with the severity of the phenotype, indicating that the selectable marker induces cis effects on neighboring genes that influence the phenotype. Homozygous mutants of all alleles had cervical skeletal defects similar to those previously reported for *Hoxb4* mutant mice. In the most severe allele, $Hoxb4^{PolIII}$, homozygous mutants died either *in utero* at approximately E15.5 or immediately after birth, with a severe defect in ventral body wall formation. Analysis of embryos showed thinning of the primary ventral body wall in mutants relative to control animals at E11.5, before secondary body wall formation. Prior to this defect, both *Alx3* and *Alx4* were specifically down regulated in the most ventral part of the primary body wall in $Hoxb4^{PolIII}$ mutants. $Hoxb4^{loxp}$ mutants in which the *neo* gene has been removed did not have body wall or sternum defects. In contrast, both the $Hoxb4^{PolIII}$ and the previously described $Hoxb2^{PolIII}$ alleles that have body wall defects have been shown to disrupt the expression of both *Hoxb2* and *Hoxb4* in cell types that contribute to body wall formation. Our results are consistent with a model in which defects in ventral body wall formation require the simultaneous loss of at least *Hoxb2* and *Hoxb4,* and may involve *Alx3* and *Alx4.*

***Key Words: Hoxb2; Hoxb4; Alx3; Alx4;* ventral body wall; genetic interaction.**

INTRODUCTION

The *Hox* gene family in the mouse consists of 39 genes encoding transcription factors that function to regulate embryonic development along the anteroposterior axis. While mutational analysis of individual *Hox* genes has provided much data about the function of these genes during embryogenesis, the sequence and expression patterns of *Hox* genes suggest that they have overlapping and synergistic functions to specify embryonic development. Analysis of mice carrying mutations in multiple *Hox* genes has confirmed this hypothesis. *Hox* genes function as highly integrated circuits such that paralogous genes, adjacent genes on the same linkage group, and even nonparalogous genes in separate linkage groups interact positively, negatively, and in parallel with each other to orchestrate the morphological regionalization of the embryo (Condie and Capecchi, 1994; Davis *et al.*, 1995; Horan *et al.*, 1995a,b; Barrow and Capecchi, 1996; Davis and Capecchi, 1996; Favier *et al.*, 1996; Fromental-Ramain *et al.*, 1996a,b; Zákány and Duboule, 1996; CHen and Capecchi, 1997, 1999; Manley and Capecchi, 1997, 1998; Gavalas *et al.*, 1998; Studer *et al.*, 1998; Barrow and Capecchi, 1999). Because *Hox* genes within a given cluster are very tightly linked, the discovery of interactions between genes has been primarily achieved by crossing strains with mutations in individual genes in the same or adjacent paralogous families, and looking for nonallelic noncomplementation or synthetic enhancement of single mutant phenotypes. Genetic interactions between genes in the same cluster have also been discovered by insertion of a strong promoter affecting the expression of neighboring genes in *cis* (Barrow and Capecchi, 1996).

Recently, a deletion encompassing *Hoxb1* through *Hoxb9* has been generated (*HoxBΔ1*) (Medina-Martinez *et*

[1] To whom correspondence should be addressed. Fax: (706) 721-8685. E-mail: nmanley@mail.mcg.edu.

0012-1606/01 $35.00

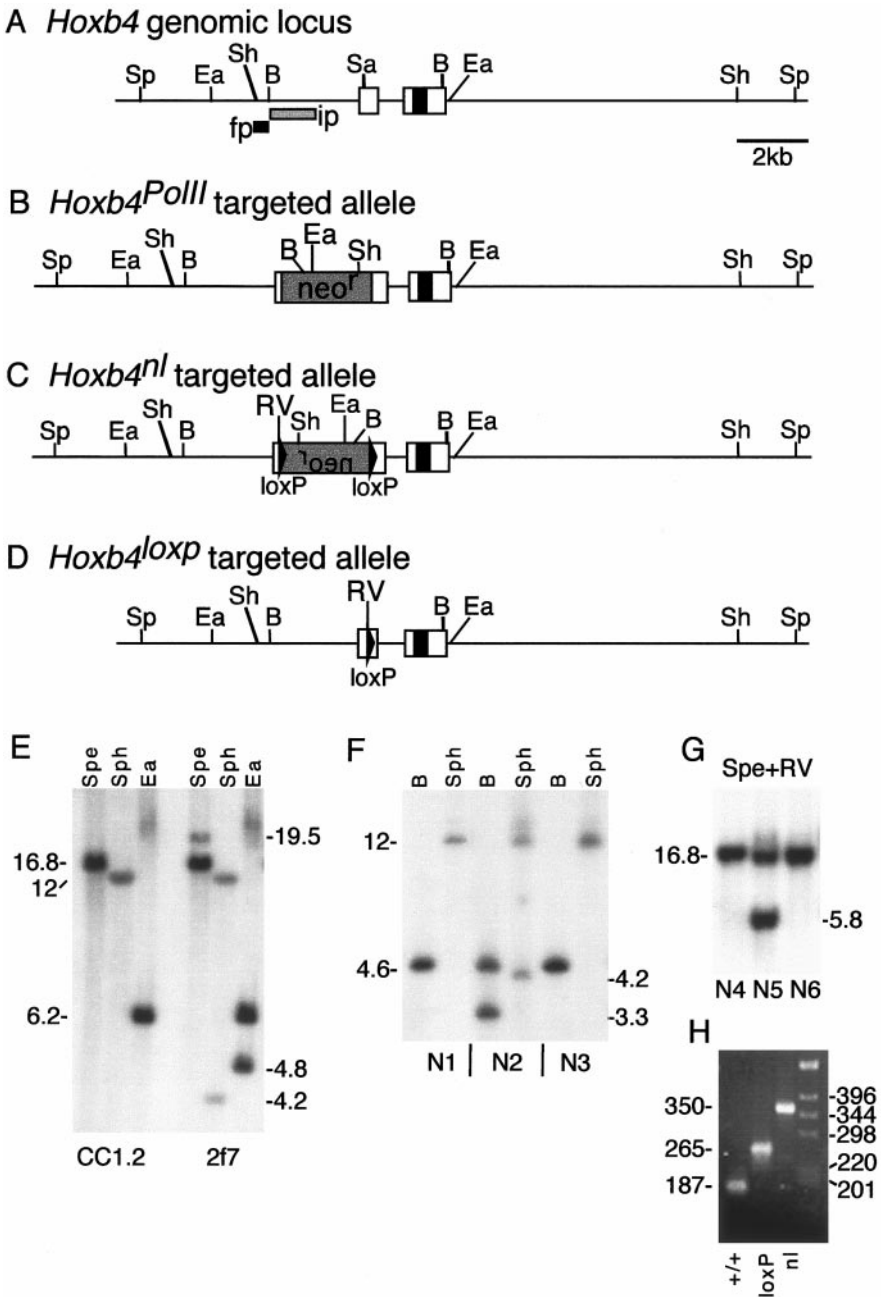

FIG. 1. Targeted disruption of the *Hoxb4* locus. (A) The *Hoxb4* genomic locus, with boxes representing the known coding exons for *Hoxb4*. Black box indicates the location of the homeobox. The locations of the flanking probe (fp) and internal probe (ip) used for analyzing targeted cell lines are shown with small boxes. Locations of restriction sites used for analysis are also shown. (B) Structure of the $Hoxb4^{PolII}$ targeted allele. Gray box indicates the inserted neo^R cassette in the first coding exon. (C) Structure of the $Hoxb4^{nl}$ targeted allele. Gray box indicates the inserted neo^R cassette in the opposite transcriptional orientation in the first coding exon, black triangles indicate the position of loxP sites flanking the neo^r cassette. (D) Structure of the $Hoxb4^{loxP}$ targeted allele. Arrow indicates the 78-bp insertion remaining, including one loxP site. (E–G) Parental band sizes (in kb) are listed on the left, mutant band sizes on the right. All bands are the expected sizes (see Materials and Methods). (E) Southern blot analysis of the CC1.2 parent cell line and a $Hoxb4^{PolII}$ targeted cell line, 2f7, using the flanking probe. (F) Southern blot analysis of tail DNA from $Hoxb4^{PolII}$ chimera offspring using the internal probe. The N2 pup is a heterozygote, the N1 and N3 littermates are wild type. (G) Southern blot analysis of tail DNA cut with *Spe*I and *Eco*RV from $Hoxb4^{nl}$ chimera offspring using the flanking probe. The N5 pup is a heterozygote, the N4 and N6 littermates are wild type. (H) PCR analysis of homozygous wild type, $Hoxb4^{loxP}$, and $Hoxb4^{nl}$ mice. Band sizes are shown to the left in base pairs; sizes of marker bands are shown to the right.

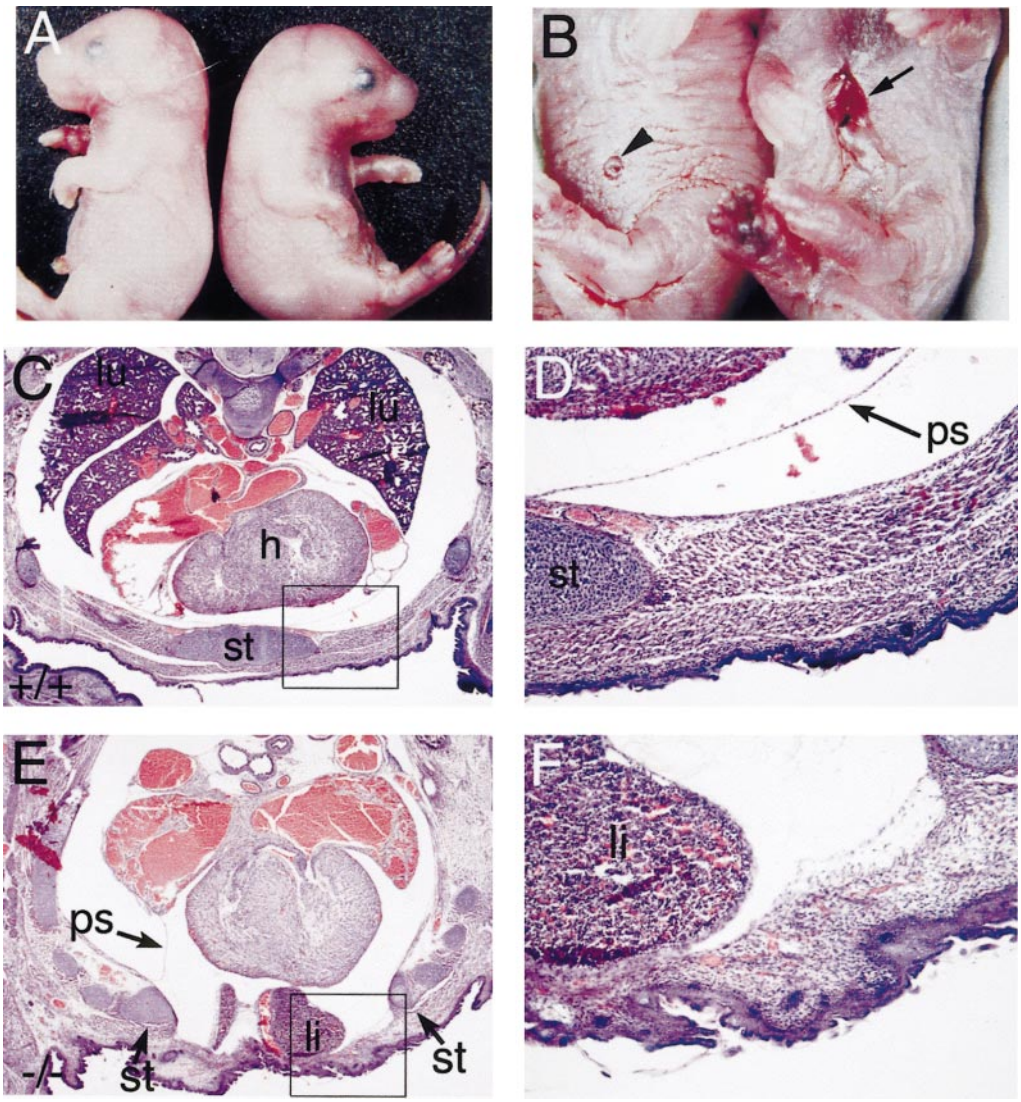

FIG. 2. Phenotype of *Hoxb4*^{PolII} mutant newborns. (A, B) Different views of the same pups, with the wild-type embryo on the left and the mutant on the right. (C–F) Transverse H&E-stained sections of newborn mice at low (C, E) and high (D, F) magnification views. High magnification views correspond to the boxes in (C) and (E). (A) Wild-type control and *Hoxb4*^{PolII} mutant newborns, lateral views. The *Hoxb4*^{PolII} mutant has a curved body shape, and appears thicker due to edema. (B) Ventral view. The wild-type embryo has a small, well-defined umbilicus (arrowhead), compared to the anteriorly displaced umbilical opening in the mutant (arrow). The ventral body wall in the mutant appears generally disorganized compared to the control. (C) Wild-type newborn chest cavity, showing heart (h), lungs (lu), and sternum (st). (D) The anterior pericardial sac (ps) is visible. Also note the presence of muscle in the body wall both lateral and ventral to the sternum. (E) *Hoxb4*^{PolII} mutant chest cavity. Although the heart view is roughly similar to that shown in (C), the trachea has just split into two bronchial tubes, and no lungs are yet visible, showing the anterior displacement of the heart. A partial pericardium is visible on the right side (ps). The dorsal rotation of the heart can be seen by comparing the location of the atria in this more posterior section with (F). A portion of the liver (li) is visible in this same section ventral to the heart, indicating diaphragmatic hernia and overall disorganization of internal organs.

al., 2000). Mice homozygous for the *HoxBΔ1* deletion showed phenotypes similar to those previously reported for the single mutants for each gene in the *HoxB* complex, although some phenotypes showed higher penetrance. The authors concluded that the *HoxBΔ1* deletion provided no evidence for synergistic interactions between *HoxB* cluster genes. However, evidence for interactions between *HoxB* genes is present in some of the existing alleles for individual *HoxB* genes. The *Hoxb2* mutant has phenotypes similar to those previously reported for targeted mutations in *Hoxb1*

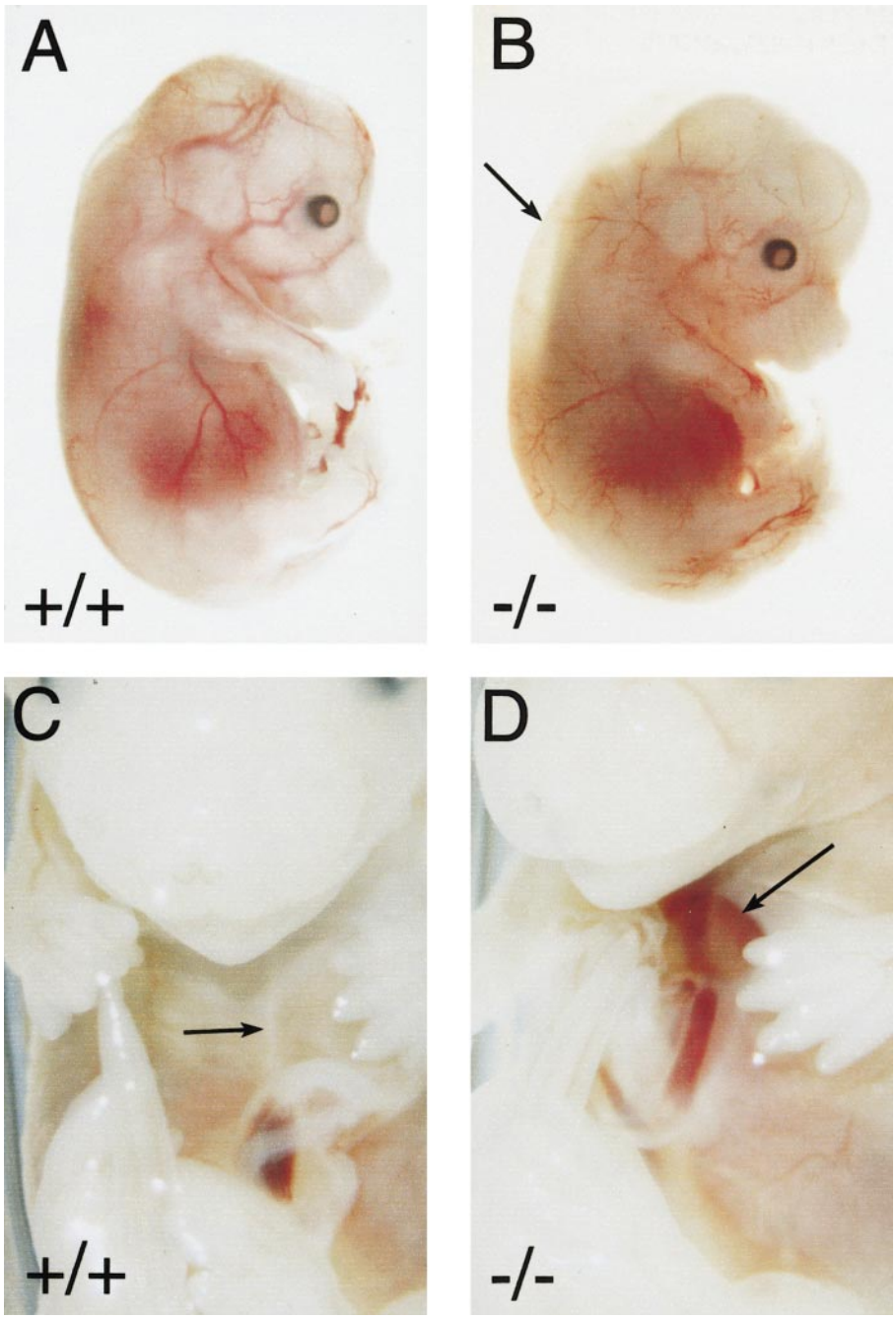

FIG. 3. *Hoxb4*^{PolII} mutant external phenotype at E15.5. (A) Lateral view of wild-type embryo. (B) A *Hoxb4*^{PolII} mutant littermate, with curved body shape and general edema, easily visible dorsally (arrow). (C) Ventral view of a wild-type embryo. The line indicating correct secondary body wall formation is clearly visible (arrow). (D) *Hoxb4*^{PolII} mutant ventral view, with an open hole in the chest through which the heart is visible (arrow).

and *Hoxb4* (Ramírez-Solis *et al.*, 1993; Barrow and Capecchi, 1996; Goddard *et al.*, 1996). Genetic analysis using a *cis-trans* test and changes in *Hoxb4* expression in the *Hoxb2* mutant suggested that the sternum phenotype could have been due in part to *cis* effects of the *neomycin resistance* (*neo*^{r}) cassette insertion into the *Hoxb2* locus. *Hoxb2* homozygous mutant embryos had loss of *Hoxb4* gene expression in the ventral body wall at E12.5. The

TABLE 1
Genotypes and Phenotypes of *Hoxb4*^{PolII} Heterozygous Intercrosses

Litter age	Total no.	+/+	+/−	−/−	No. (%) −/− found dead	No. with unfused sternum	No. with open body wall
Newborn	175	54	112	18	16 (90%)	16	0
E18.5	39	14	14	11	1 (10%)	11	0
E15.5	46	10	22	14	5 (36%)	9[a]	4[a]
E14.5	21	6	11	4	0	4	3
E13.5	42	5	23	14	0	—[b]	2[c]
E11.5	20	9	4	7	0	—	0

[a] Some dead embryos were being resorbed and could not be scored for this phenotype.
[b] The sternum normally fuses at E14–E14.5.
[c] Seven additional embryos had visibly thin body walls compared to littermates.

results from this study suggested that loss-of-function of both *Hoxb2* and *Hoxb4* contribute to malformation of the sternum. In fact, the phenotypes of two previously reported alleles for *Hoxb4* also suggested that mutation of *Hoxb4* alone was insufficient to cause sternal defects, although other differences between the alleles left open other explanations as well (Ramírez-Solis *et al.*, 1993).

In this report, we use an allelic series of three *Hoxb4* mutants, *Hoxb4*^{PolII}, *Hoxb4*^{nl}, and *Hoxb4*^{loxP}, to investigate the role of *HoxB* genes in ventral body wall development. The *Hoxb4*^{PolII} and *Hoxb4*^{nl} alleles carry insertions of a *neo*^{r} cassette in opposite orientations in the first exon. The *Hoxb4*^{PolII} mutant has complete failure of sternal fusion, poor and/or delayed body wall formation, and embryonic or perinatal lethality. The *Hoxb4*^{nl} allele, with the *neo*^{r} gene in the opposite transcriptional orientation, has a similar phenotype but at lower penetrance and severity. In the *Hoxb4*^{loxP} allele, the *neo*^{r} cassette has been removed from *Hoxb4*^{nl} by cre-mediated recombination. The *Hoxb4*^{loxP} strain has no body wall defects, confirming that loss of the *Hoxb4* gene alone cannot mediate these defects and that the body wall defects are associated with *cis* effects of the inserted *neo*^{r} cassette. Similarly, a *Hoxb2* allele in which the selectable marker has been removed has normal body wall formation. Taken together, these results indicate that loss of at least two *Hox* genes, *Hoxb2* and *Hoxb4*, is required to develop a sternal defect. The phenotype of the *Hoxb4*^{PolII} allele is more severe than that of the previously published alleles of *Hoxb2* or *Hoxb4* with respect to body wall and sternal defects (Ramírez-Solis *et al.*, 1993; Barrow and Capecchi, 1996). Analysis of the embryonic phenotypes of mutants where the function of *Hoxb4* and *Hoxb2* are simultaneously disrupted indicates that the sternum defects are due to abnormalities in the development of both the primary and secondary body walls. Marker gene analysis of the *aristaless* homologs *Alx3* and *Alx4* showed a specific loss of these genes in the ventral body wall of *Hoxb4*^{PolII} mutant embryos prior to a morphological defect. As mutation of *Alx4* is associated with defects in sternal closure, this result suggests a molecular mechanism for the observed defects.

MATERIALS AND METHODS

Targeting Vector Construction

Genomic DNA (10.6 kb) containing the *Hoxb4* locus was isolated from an embryo-derived stem (ES) cell genomic library and used to construct the targeting vector. The vector included 2.3 kb of sequences upstream of the first coding exon, and extended to an *Eco*RI site 6 kb downstream of the *Hoxb4* gene. In the *Hoxb4*^{PolII} allele, the first coding exon was disrupted by insertion of the KT3NP3 cassette in the same transcriptional orientation as *Hoxb4* at the *Sal*I site located 39 bp from the initiation codon. The KT3neo cassette contains the *neomycin resistance* gene (*neo*^{r}) under control of the PolII promoter (Deng *et al.*, 1993; Barrow and Capecchi, 1996). The *Hoxb4*^{nl} allele was constructed similarly, but the *neo*^{r} cassette was flanked by loxP sites and inserted in the opposite transcriptional orientation as *Hoxb4*. The final targeting vectors contained the 10.6 kb of genomic DNA including the mutated allele, flanked by the *TK1* and *TK2* herpes simplex virus *thymidine kinase* genes.

Generation of Hoxb4 Mutant Mice

The *Hoxb4*^{PolII} targeting vector was linearized and electroporated into CC1.2 ES cells. The *Hoxb4*^{nl} targeting vector was linearized and electroporated into R1–45 ES cells. Electroporated cells were cultured by using positive/negative selection in G418 and FIAU (Mansour *et al.*, 1988). Clones containing a correctly targeted allele of *Hoxb4* were identified by Southern blot analysis (Fig. 1). Fidelity of the homologous recombination events were confirmed by Southern blot analysis with four restriction enzymes, using 5′ and 3′ flanking probes and a probe specific for the *neo*^{r} gene (Fig. 1 and data not shown). For *Hoxb4*^{PolII}, 7 out of 91 CC1.2 ES cell lines were obtained with correctly targeted mutations. Two of these cell lines were used to generate germline chimeras. For *Hoxb4*^{nl}, 2 of 133 ES cell lines were correctly targeted, one of which was used to generate germline chimeras. Positive cell lines for both constructs were injected into C57BL6 blastocysts. Male chimeras were backcrossed to C57BL6 females, and offspring derived from ES cells

were identified by coat color and genotyped by Southern blot analysis or PCR (Figs. 1E–1H, and see below). Mice identified as heterozygous for the *Hoxb4* mutation were intercrossed to expand the colony and generate *Hoxb4* homozygous mutants.

To generate a strain that does not carry a *neo*^{r} cassette, *Hoxb4*^{nl} heterozygotes were intercrossed and fertilized eggs were collected and injected with a cre expression vector (Araki *et al.*, 1995). Progeny in which the cre-mediated deletion had taken place were identified by PCR, followed by sequencing (Fig. 1H, see below). The resulting deleted strain was designated the *Hoxb4*^{loxP} strain.

Litters from each of the three mutant strains were collected for analysis either during gestation, on the day of birth, or at weaning to assess viability. Embryonic age was estimated by considering noon of the day of a vaginal plug as E0.5, and confirmed by counting somites.

Genotype Analysis for Hoxb4 Alleles

Mice and embryos were genotyped by either Southern blot or PCR analysis of tail or yolk sac DNA. For Southern blot analysis of *Hoxb4*^{PolII} (Figs. 1E and 1F), genomic DNA was digested with restriction enzymes and probed with either flanking or internal probes (fp or ip, Fig. 1A). Restriction fragments sizes generated were as follows: *Spe*I—wild type 16.8 kb, mutant 19.5 kb; *Sph*I—wild type 12 kb, mutant 4.2 kb; *Eag*I—wild type 6.2 kb, mutant 4.8 kb; *Bam*HI (ip only)—wild type 4.6 kb, mutant 3.3 kb. Southern analysis of *Hoxb4*^{nl} was performed using the 5′ fp and genomic DNA digested with *Spe*I and *Eco*RV (Fig. 1G), giving a 16.8-kb wild-type band and a 5.8-kb mutant band.

PCR analysis for all alleles was performed in 20-μl reactions amplified for 34 cycles with 10 seconds at 94°C, 20 seconds at 65°C, and 30 seconds at 72°C. Two *Hoxb4*-specific PCR primers and one *neo*^{r} gene-specific primer were used to genotype animals. The *Hoxb4*-specific primers were the 5′ primer, located immediately 5′ of the initiation codon, 5′-TTTTGTGGGCAATTCCCAGAAATT-3′ [nucleotides −25 to −2, (Graham *et al.*, 1988)]; and the 3′ primer, located 120 bp 3′ of the *Sal*I site, 5′-AAAGGCC-GCCTCCGGCTGGAAGCC-3′ (nucleotides 162-139). The *neo*^{r} gene specific primer used was located on the anti-sense strand 174 bp inside the 5′ end of the KT3NP3 cassette, 5′-CGTTCAT-GAATATTCAGTTCACCGCTGA-3′ The 5′ and 3′ primers gave a 187-bp product for the wild-type allele, and a 265-bp product for the *Hoxb4*^{loxP} allele (Fig. 1H). The 5′ and neo-specific primers gave a 238-bp product for the *Hoxb4*^{PolII} mutant allele, and a 350-bp product for the *Hoxb4*^{nl} allele (Fig. 1H and data not shown). PCR products were analyzed by using agarose or polyacrylamide gel electrophoresis.

Histology

For paraffin sectioning, embryos from timed matings or newborn mice were fixed in 4% formaldehyde in phosphate buffered saline (PBS) and embedded in Paraplast X-tra. Sections (10 μm) were stained with hematoxylin and eosin (H&E) and mounted in DPX. Whole-mount stained embryos were processed for paraffin sectioning at 6–10 μm and counterstained with Nuclear Fast red as previously described (Manley and Capecchi, 1995). Sections were photographed by using a Spot digital camera and an Olympus BX-60 microscope.

RNA in Situ Hybridization

Whole-mount *in situ* hybridizations were performed as described (Carpenter *et al.*, 1993; Manley and Capecchi, 1995). The *Hoxb2*, *Hoxb3*, *Hoxb5*, and *AP-2* probes used were previously described (Manley and Capecchi, 1995; Rancourt *et al.*, 1995; Rossel and Capecchi, 1999). The *Alx3* probe was derived by PCR amplification of a 950-bp fragment from the 3′ end of the gene, including the last 309 bp of coding sequence. The *Alx4* probe was derived by PCR amplification of a 497-bp fragment from the 3′ end of the gene, including the last 155 bp of coding sequence. Staged mouse embryos were fixed overnight in 4% formaldehyde in PBS, dehydrated into methanol, and stored at −20°C until use. The digoxigenin-labeled RNA probes were used at 0.5 μg/ml. Alkaline phosphatase-conjugated anti-digoxigenin Fab fragments were used at 1:5000. Color reactions were carried out for 2–15 h. Embryos were photographed without clearing with Ektachrome 160T film on a Ziess SV11 dissecting microscope.

RESULTS

An Allelic Series for the Hoxb4 Locus

The targeting vectors for the *Hoxb4*^{PolII} and *Hoxb4*^{nl} alleles were constructed by inserting the *PolIIneopA* cassette into the *Sal*I site in the first exon, 39 bp from the initiation codon (Fig. 1). The orientation of the *neo* cassette is opposite for the different alleles (see Fig. 1). This *Sal*I is the same restriction site used to generate the *Hoxb4*^{r} allele previously reported (Ramirez-Solis *et al.*, 1993), although the promoter used to drive *neo* expression is different (PolII vs. PGK). In the *nl* strain, the *neo* cassette was flanked by *loxP* sites. Cre-mediated deletion of the *neo* cassette in *Hoxb4*^{nl} generated the *Hoxb4*^{loxP} strain, containing a 78-bp insertion after codon 12 of *Hoxb4* that has a stop codon in frame with the *Hoxb4* transcript.

Frequency and Severity of Body Wall Defects in Hoxb4 Mutants Corresponds to the Presence and Orientation of the neo Cassette

Heterozygous mice for all alleles appeared normal, with 100% viability and fertility. No *Hoxb4*^{PolII} homozygous mutants (0/89) were identified in weanling mice (Table 1). At the newborn (NB) stage, 18 of 175 (10%) were homozygous mutants, 16 of which were dead or dying immediately after birth. The two remaining homozygous mutants were processed for sectioning or skeleton preps and were found to have defective yet fused sternums (not shown). The *Hoxb4*^{PolII} mutants had increased body curvature, but had no defects in the vertebral column that could account for this difference (Figs. 2A and 2B and not shown). Of the 16 NB pups found dead, all had completely unfused sternums. Skeletal abnormalities in the cervical vertebrae and sternum were similar to the most severe mutant phenotype previously described for the *Hoxb4*^{r} allele (Ramírez-Solis *et al.*, 1993). Three mutants found dead at birth were much smaller than littermates and extremely pale. These pups appeared to have died *in utero* late in gestation.

In comparison to the *Hoxb4*^{PolII} mutants, *Hoxb4*^{nl} homozygotes had similar body wall defects, but at a lower frequency. *Hoxb4*^{nl} homozygote newborns were obtained at

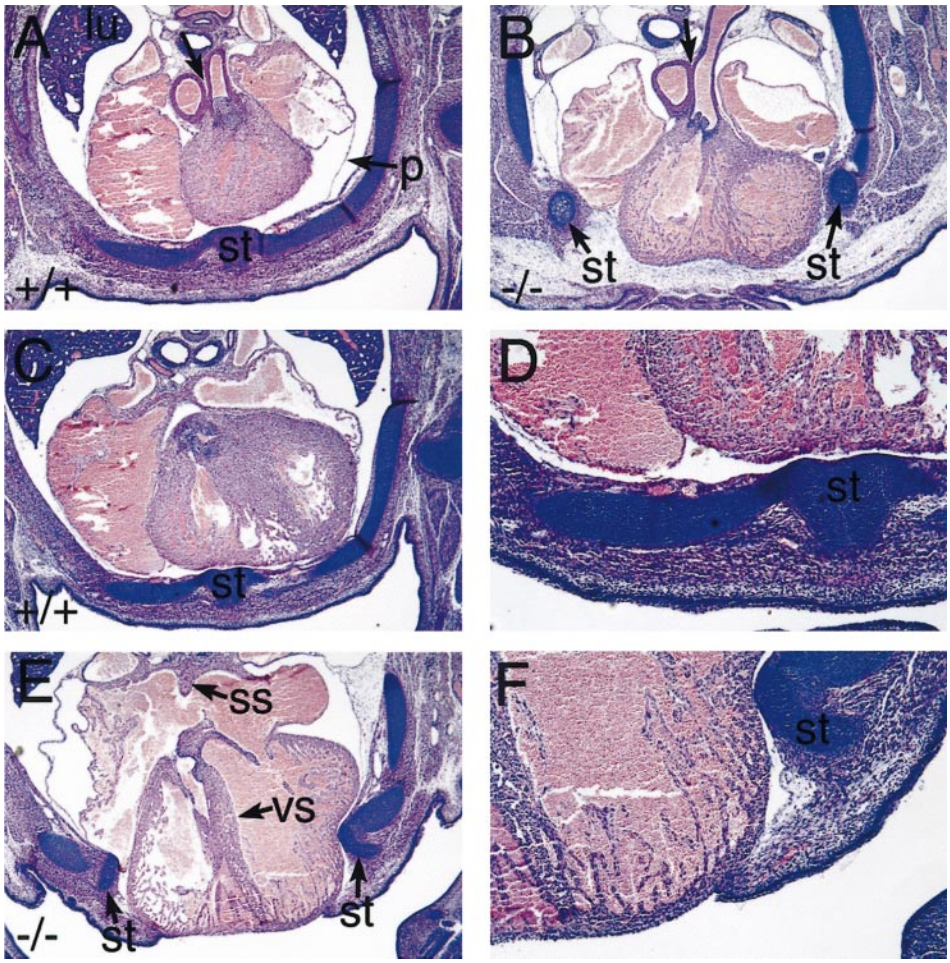

FIG. 4. Normal ventricular and great vessel septation, but severe body wall defects in *Hoxb4*^{PolII} mutant embryos at E15.5. Transverse H&E stained sections of newborn mice at low (A, C, E) and high (B, D, F) magnification views. (A) Wild-type embryo showing outflow septation (arrow), and closed sternum (st). The pericardium (p) and lungs (lu) are also visible in this section. (B) *Hoxb4*^{PolII} mutant with unfused, laterally located sternabrae (st). This embryo has normal outflow septation (arrow), thinned ventricular walls and septum, and an enlarged heart. There is no visible anterior pericardium. Note that the lungs are not visible, indicating anterior displacement of the heart. The heart is embedded in edematous mesenchyme ventrally. There is no musculature past the laterally displaced sternal bars. (C, D) Section of a wild-type embryo at approximately the middle of the chest cavity, showing the heart, chest wall, and fused sternum. (E, F) Sections of the same *Hoxb4*^{PolII} mutant embryo shown in (B) at a more caudal level, showing a large hole completely through the chest wall. The heart is dilated and squeezed between the unfused sternal bars (st). The ventricle walls are thin and poorly developed, but the septum is intact. The atria are still connected by the foramen ovale, but the septum secundom is forming normally.

the expected frequency, and 32 of 78 (41%) had a split sternum. Thus, although the size and nature of the *neo* cassette were essentially identical between the *PolII* and *nl* strains, the orientation of the *neo* cassette appears to have a dramatic effect on sternal development. Removal of the *neo* cassette in *Hoxb4*^{loxp} mutants completely eliminated the split sternum phenotype (0/31 homozygotes). However, the defects in cervical vertebrae were the same in all three strains (not shown). These results indicate that the sternum and body wall defects in the *Hoxb4*^{PolII} and *Hoxb4*^{nl} homozygotes were due at least in part to *cis*-acting effects of the inserted *neo* cassette on neighboring genes. In contrast, the cervical vertebral defects were entirely due to loss of *Hoxb4*.

Hoxb4^{PolII} *Homozygotes Have Extensive Defects in the Ventral Body Wall*

As the *Hoxb4*^{PolII} homozygotes had the most severe and highly penetrant phenotype, they were examined in more detail. External examination of the NB mutants showed a number of defects in the ventral body wall (Figs. 2A and 2B). The umbilical opening was anteriorly displaced, poorly organized, and unusually large. The overall anterior–

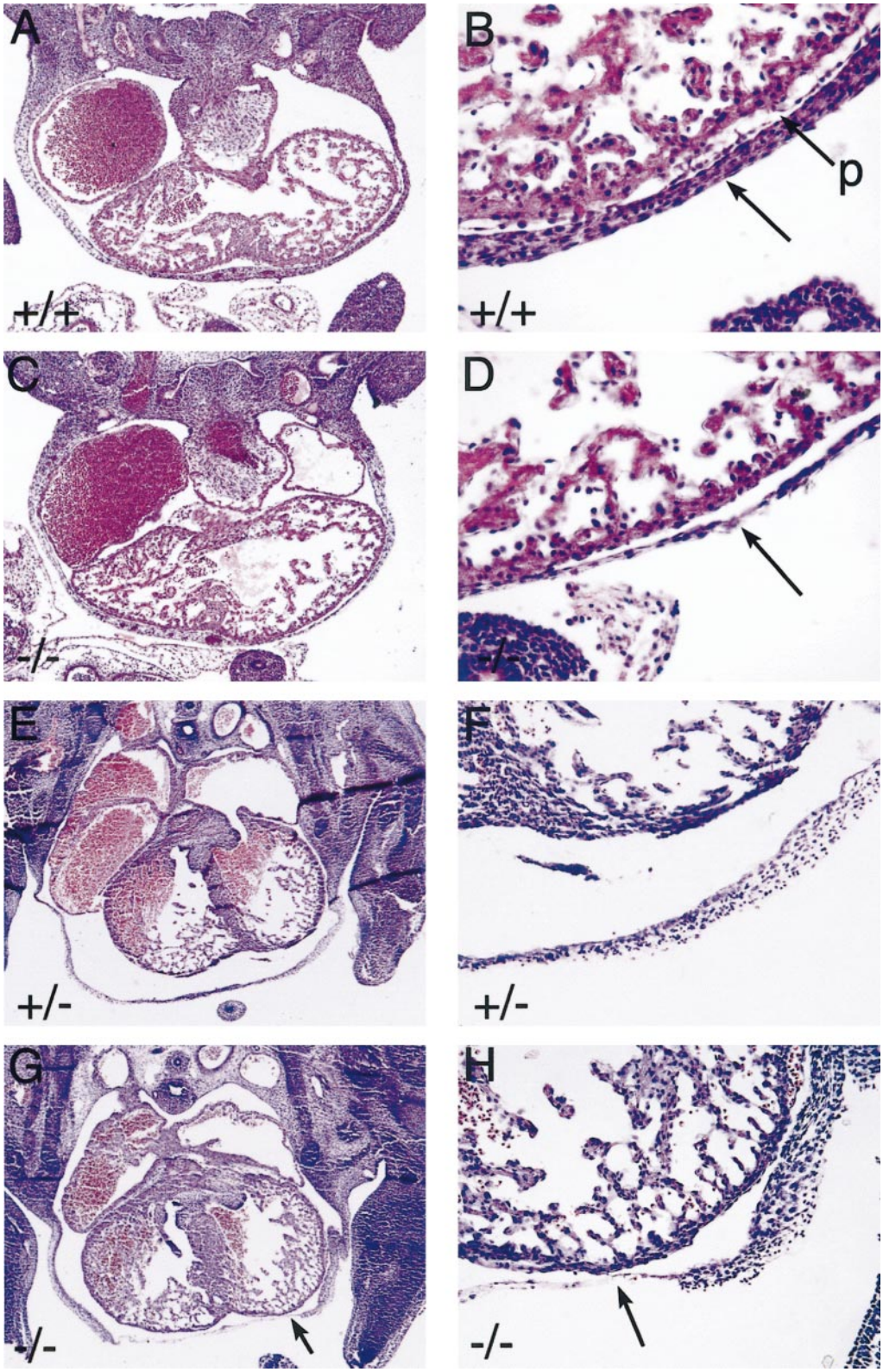

FIG. 5. Defect in the primary body wall at E11.5 and E13 in *Hoxb4*^{PolII} mutants. Transverse histological sections through the thoracic region of E11.5 (A–D) and E13 (E–H) embryos stained with H&E. High magnification views on the right, are of the same sections shown on the left. (A) Wild-type E11.5 embryo with normal primary body wall development. (B) The pericardium (p) is developing between the ventricle and the body wall (arrow). (C) E11.5 *Hoxb4*^{PolII} homozygous mutant embryo has a thinner ventral primary body wall compared to the littermate control; more lateral regions are comparable to wild type. The heart is normal. (D) No pericardium is visible at higher magnification, and the body wall (arrow) is only 1–2 cells thick. (E, F) E13 *Hoxb4*^{PolII} heterozygote with an intact primary body wall. The sternal rudiments, ribs, and musculature that will form the secondary body wall are still far lateral. (G, H) E13 *Hoxb4*^{PolII} mutant with a deteriorating primary body wall. The most ventral portion is extremely thin (arrow). The components of the secondary body wall are similar to the control.

posterior length of the abdominal wall was shortened. Dying *Hoxb4*^{PolII} mutant homozygous newborn (NB) pups had obvious difficulty breathing and a collapsed or funnel chest resulting from the unfused sternum. Histological examination of newborn homozygotes showed only skin and loose mesenchyme covering the chest cavity, with skeletal and muscular components located laterally (Fig. 2F). The pericardium was missing or incomplete, and the diaphragm was poorly formed. There was also a general derangement of the internal organs. The heart was anteriorly displaced and rotated in the dorsal–ventral axis, such that the atria were dorsal to the ventricles (Fig. 2E). Visceral organs (liver, small intestines) were in some cases located ventral to the heart, protruding through a diaphragmatic hernia (Figs. 2E and 2F). It is likely that this disorganization of the body cavity was secondary to defects in body wall formation and failure of sternal fusion.

Many Hoxb4^{PolII} *Mutants Die in Mid- to Late Gestation*

The number of recovered *Hoxb4*^{PolII} homozygous mutant NB pups was only 40% of the number expected, suggesting some embryonic lethality. We collected litters at various stages from E11.5 to E18.5 to look for embryonic lethality and to determine the embryonic origins of the observed defects (Table 1). At E15.5, 5 of 14 (36%) mutant embryos recovered were dead. All mutant embryos had unfused sternums, more than half were notably edematous, and some had openings in the body wall over the heart (Table 1 and Figs. 3B and 3D). At E14.5, all four mutants observed had an unfused sternum. Three of these also had a hole in the chest wall, and were noticeably edematous. Even at E13.5, before sternal fusion normally occurs, 9 of 14 *Hoxb4*^{PolII} mutant embryos examined by dissection had open or visibly thinner ventral body walls compared to heterozygous and wild type littermates (Table 1). Taken together, these data indicate that most if not all *Hoxb4*^{PolII} mutants have defective body walls even before sternal migration and fusion, which normally occurs at E14.5. Embryos possessing the most severe body wall defect, persistent opening in the body wall, died *in utero* at around E15.5. Because we never recovered mutants with this severe defect following this stage, we conclude that development beyond E15.5 requires a closed body wall. In contrast, those mutants that succeed in closing the body wall appear capable of surviving beyond this block to birth. At least 90% of these mutants, however, still have severe body wall malformations, and die at or soon after birth.

Heart Defects in the Hoxb4^{PolII} *Mutants*

As the edema indicated possible hemodynamic stress and the lethality at E15.5 of some *Hoxb4*^{PolII} embryos is similar to that seen in mice with defects in cardiac septation (persistent truncus arteriosus, ventricular septal defects), we examined *Hoxb4*^{PolII} mutants for heart defects at E15.5 (Fig. 4). Outflow tract septation was normal, indicating that there were no neural crest-associated heart defects (Fig. 4B). Ventricles of mutant embryos were dilated, and both the ventricular walls and the ventricular septum were thin and poorly developed (Figs. 4E and 4F). In the majority of cases where the sternum was not fused, the heart protruded through the two sternal bars (Figs. 4B, 4E, and 4F). In the one case of a *Hoxb4*^{PolII} homozygote with a closed but abnormally fused sternum that was examined histologically, the heart appeared normal (not shown). As the degree of heart dilation and edema was correlated with the severity of the defect in the body wall, we conclude that the observed heart defects are likely to be secondary to defects in formation of the chest cavity.

Hoxb4^{PolII} *and Hoxb2*^{PolII} *Mutants Have Defects in Primary Body Wall Development*

To determine whether the defect was in the primary or secondary body wall, we examined embryos at early stages of primary body wall formation. No differences were seen between mutants and controls at E10.5–E11 (not shown). At E11.5, the primary body wall in *Hoxb4*^{PolII} homozygous embryos was thinner than littermate wild-type controls, particularly in the most ventral region (Fig. 5). This thinning was pronounced in two of three embryos analyzed at this stage, and less dramatic but still present in the third (not shown). The defect in pericardium formation was also seen at this stage (compare Figs. 5B and 5D). By E13, the most ventral portion of the primary body wall was extremely thin for much of the antero-posterior axis in all *Hoxb4*^{PolII} mutants examined (Figs. 5G and 5H). Apoptosis was not increased in the ventral body wall at E12.5–E13.5, suggesting that this was not the mechanism for the observed thinning (data not shown). On the other hand, the sternal rudiments and mesodermal components of the secondary body wall appeared normal at this stage, and were distal from the site of this malformation. These data indicated that the initial defect in these mutants is in the transition from the primary to the secondary body wall.

The previously described *Hoxb2*^{PolII} mutant contains the same *neo* cassette as the *Hoxb4*^{PolII} mutants, and has a similar, although less severe, NB sternum defect (Barrow and Capecchi, 1996). We investigated whether these phenotypes had a common embryonic origin. In *Hoxb2*^{PolII} mutants at E13.5, we saw thinning in the body wall identical to *Hoxb4*^{PolII} mutants (Figs. 6C–6F). However, in contrast to *Hoxb4*^{PolII} mutants, not all *Hoxb2*^{PolII} mutants showed this defect, and the lateral extent of the thinned region was variable in *Hoxb2*^{PolII} mutant embryos (compare Figs. 6C and 6E). The embryonic phenotypes are consistent with the *Hoxb2*^{PolII} and *Hoxb4*^{PolII} newborn phenotypes. All *Hoxb4*^{PolII} mutant embryos examined showed extensive thinning and/or holes in the body wall, and >90% of *Hoxb4*^{PolII} mutants have a severe phenotype at the newborn stage. The *Hoxb2*^{PolII} mutant embryonic phenotype was more variable both in extent and frequency, and the split

sternum phenotype at birth was also less severe and more variable in $Hoxb2^{PolII}$ mutants than in $Hoxb4^{PolII}$ mutants. Taken together, these results are consistent with the presence and lateral extent of the thinned region during midgestation dictating the severity of the body wall defect. These data also suggest that the mechanisms of the body wall defects are very similar if not identical in the $Hoxb2^{PolII}$ and $Hoxb4^{PolII}$ mutants.

Severity of the Hoxb4 Mutant Phenotype Corresponds to Effects on Hoxb2 Expression

Our current and previous genetic and gene expression data suggest that the presence and severity of the split sternum defect in *Hoxb4* mutants is related to the effect of the neo^r cassette on the expression of neighboring *Hox* genes, including *Hoxb2*. We have previously shown that *Hoxb2* expression is largely absent from rhombomere 6 (r6) and its associated migrating neural crest cells (NCC) in $Hoxb4^{PolII}$ mutants (Barrow and Capecchi, 1996). If the loss of *Hoxb2* expression in r6 NCC is involved in the phenotype, we would expect that in the $Hoxb4^{loxP}$ allele, which does not have a body wall defect, *Hoxb2* expression would be normal. Consistent with this hypothesis, *Hoxb2* expression is not affected in $Hoxb4^{loxP}$ mutants (data not shown). Also, preliminary analysis of an allele of *Hoxb2* in which the selectable marker has been removed shows that this allele is viable and does not have any obvious body wall defects (Zhang and Capecchi, unpublished results). These results support the conclusion that the defects in body wall development in these mutants are the result of simultaneous effects on the transcription of at least two *Hox* genes, *Hoxb2* and *Hoxb4*.

We also investigated whether the expression of other neighboring *Hox* genes was affected in *cis* by the $Hoxb2^{PolII}$ or $Hoxb4^{PolII}$ mutations. *Hoxb5* expression was normal at E12.5 in both $Hoxb2^{PolII}$ and $Hoxb4^{PolII}$ mutant embryos (data not shown). *Hoxb3* is expressed strongly in the ventral body wall at E12.5 (Fig. 7A), and is still present at this site in $Hoxb4^{PolII}$ mutants (although the expression domain appears thinner due to the thinning of the body wall in these mutants at this stage) (Fig. 7B). In contrast, in $Hoxb2^{PolII}$ mutant embryos *Hoxb3* expression begins normally but then is lost or strongly reduced in the ventral body wall at E12.5 (Fig. 7C). Since *Hoxb3* expression is not changed in the $Hoxb4^{PolII}$ mutants, and the *Hoxb3* single mutant does not affect sternum or body wall development (Manley and Capecchi, 1997), we conclude that the reduced *Hoxb3* expression seen in $Hoxb2^{PolII}$ mutants is not critically involved in the development of the body wall defect. However, we cannot exclude the possibility that there are other effects on *HoxB* gene expression not detected by this analysis.

Neural Crest Cell Migration Appears Normal

To determine whether the loss of *Hoxb2* expression in r6 NCC was due to failure of r6 NCC migration, we used *AP-2* as a marker for all migrating NCC at E9.0–E9.5 (21–25 somites (Zhang *et al.*, 1996). *AP-2* expression in $Hoxb4^{PolII}$ mutants was indistinguishable from controls, indicating that r6 NCC were present and migrating normally (Figs. 7D and 7E). Therefore, the observed morphological defects in the ventral body wall were not due to failure of NCC migration.

Alx3 and Alx4 Are Down Regulated in the Ventral Body Wall in $Hoxb4^{PolII}$ Mutant Embryos

We used *Alx3* and *Alx4* as molecular markers for the ventral body wall. At E10.5–E11, *Alx3* and *Alx4* are expressed in neural crest-derived mesenchyme and lateral plate mesoderm, including the ventral body wall, flank mesoderm, and pharyngeal arches (Figs. 7F and 7G; data is shown for *Alx3*) (Qu *et al.*, 1997; ten Berge *et al.*, 1998). There were no differences in *Alx3* and *Alx4* expression in control and $Hoxb4^{PolII}$ mutant embryos at E10.5 (not shown). However, both *Alx3* and *Alx4* are down regulated in the most ventral body wall in $Hoxb4^{PolII}$ mutants at E11, just prior to the appearance of a morphological defect in this structure (Figs. 7H and 7I; data is shown for *Alx3*). Other sites of expression, including flank mesoderm, were not affected. As mutation of *Alx4* (in combination with *Cart-1*, another *aristaless* family member) has been shown cause sternum closure defects (Qu *et al.*, 1999), loss of *Alx3* and *Alx4* may be involved in mediating the ventral body wall defect in these mutants.

DISCUSSION

Hoxb2 and Hoxb4 Are Both Required for Proper Formation of the Ventral Body Wall

An allelic series provides a valuable system to investigate the interactions between *Hox* genes in the same cluster. Mice that are homozygous for various alleles of *Hoxb2* and *Hoxb4* exhibit split sternum defects at varying penetrance. This phenotype is only observed in alleles with effects on neighboring *HoxB* genes, particularly where the expression of *Hoxb2* and *Hoxb4* is simultaneously affected in cell types that can contribute to the ventral body wall (this report and Barrow and Capecchi, 1996). Mice homozygous or trans-heterozygous for these alleles possess body wall defects. Conversely, mice with small frame shift mutations in the first ($Hoxb4^{loxP}$) or second ($Hoxb4^{s}$) exon of *Hoxb4* or in *Hoxb2* possess normal sternums. These results demonstrate that loss of either *Hoxb4* or *Hoxb2* function alone is not sufficient to disrupt normal body wall development. Therefore, the simplest interpretation of our genetic and gene expression data is a model in which *Hoxb2* and *Hoxb4* are redundant for this function. These data do not, however, exclude the possibility that additional genes in the *HoxB* cluster are also involved in generating the phenotype.

Hoxb2 and *Hoxb4* alleles with effects on neighboring *HoxB* genes can have severe defects in body wall formation.

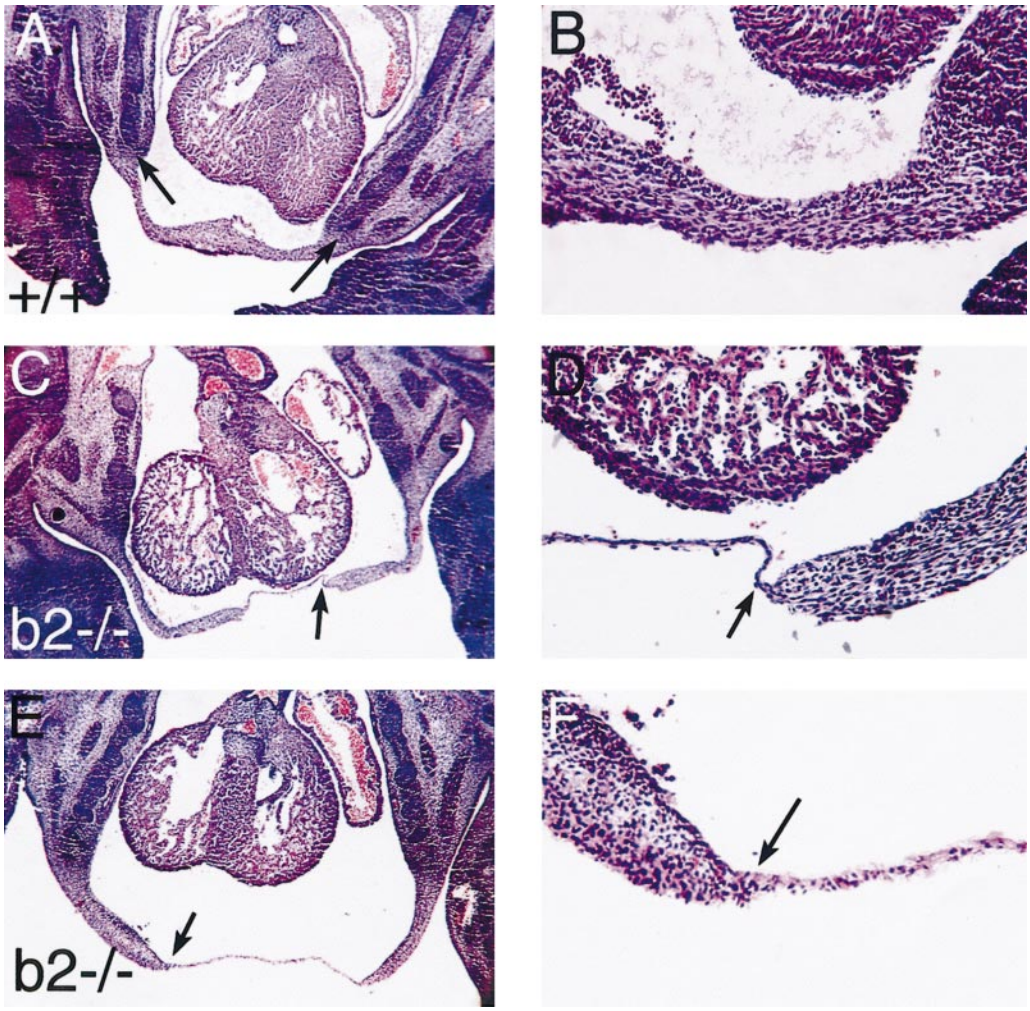

FIG. 6. Variable lateral extent of body wall defects in *Hoxb2*$^{-/-}$ embryos. Transverse histological sections through the thoracic region of E13.5 embryos at low (A, C, E) and high (B, D, F) magnification views. Embryos are slightly older than those shown in Fig. 6. (A, B) Control embryo with a well developed primary body wall; the arrows indicate the location of the components of the secondary body wall (muscle, sternal bars, ribs). (C, D) *Hoxb2* mutant embryo; note that the thinning in the body wall is similar to that seen in the *Hoxb4*^{PolII} mutant in Fig. 5, but is less extensive. Arrows indicate the boundary between normal and thinned tissue. (E, F) A second *Hoxb2* mutant; the thinning in the ventral body wall is comparable to the *Hoxb4*^{PolII} mutant in Fig. 5.

In the most severe allele, *Hoxb4*^{PolII}, defects in primary body wall development originate as early as E11.5 and lead to failure of secondary ventral body wall closure at E13.5–E14.5. If the defect is not overcome by E15.5–E16.5 the embryos die, although at least 50% progress to closure of the body wall and survive to birth. At birth, they then succumb due to the severe defects in the structure of the chest cavity, preventing proper cardio-pulmonary function.

Comparison of Hoxb4 Mutant Alleles and the Hox B Cluster Deletion

A previously published study of *Hoxb4* mutants generated two different *Hoxb4* alleles, *Hoxb4*^{r} and *Hoxb4*^{s} (Ramirez-Solis *et al.*, 1993). *Hoxb4*^{r} contained an insertion of a *PGK-neo*^{r} cassette into the first exon of *Hoxb4,* and *Hoxb4*^{s} had a point mutation in the homeobox causing premature termination. Similar to our results, presence of the selectable marker corresponded to defective sternal development. Since the *Hoxb4*^{r} and *Hoxb4*^{s} alleles were constructed at different sites in the gene, the authors were unable to determine the exact cause of the different phenotypes in the two alleles, although effects of the PGK promoter on neighboring *Hox* genes was one possible explanation given. Our current data provides additional evidence that the *Hoxb4*^{loxP} and *Hoxb4*^{s} alleles are both *Hoxb4* null alleles, showing that there is no function for *Hoxb4* that does not involve the DNA binding domain, and that

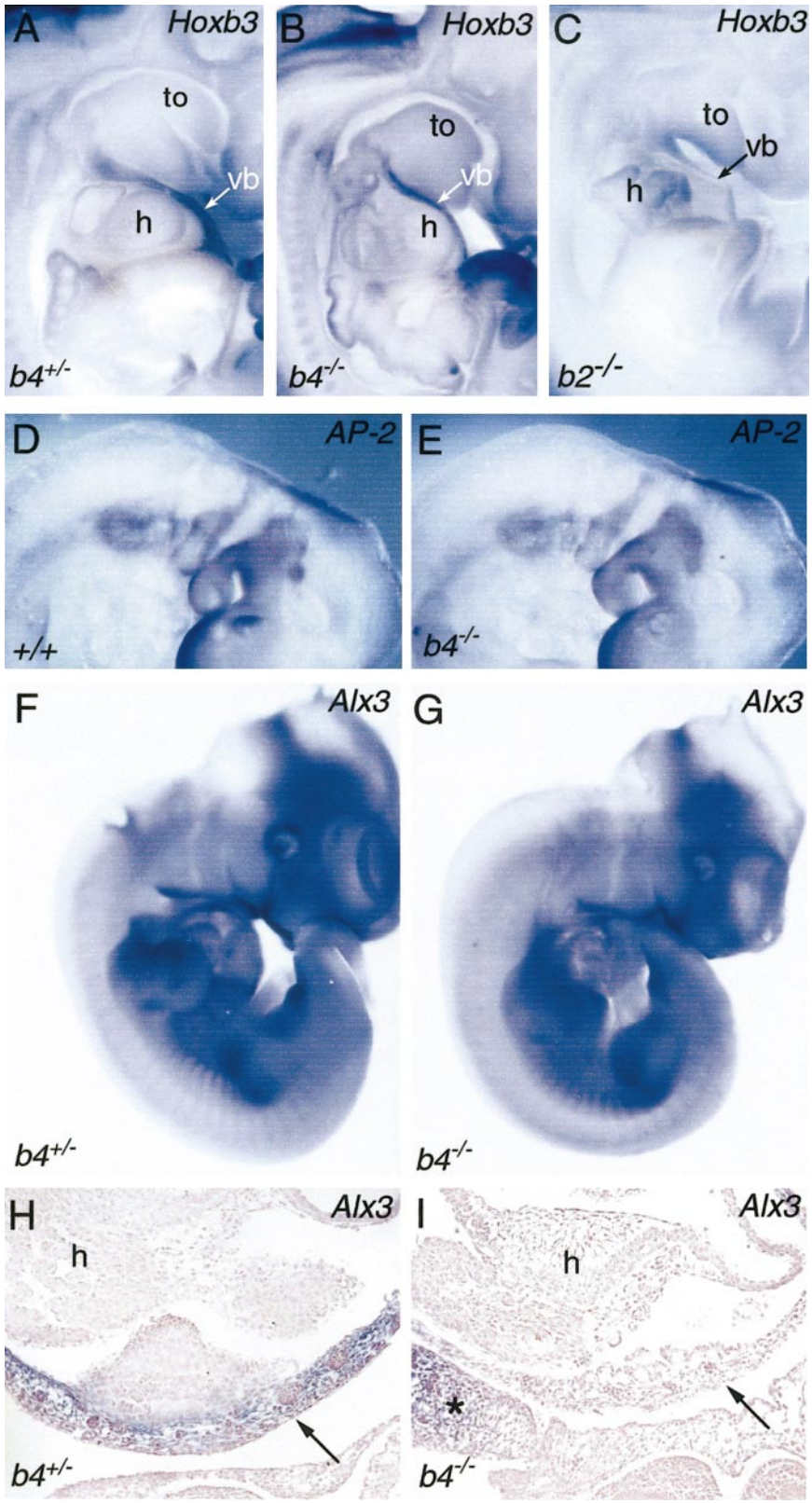

FIG. 7. RNA *in situ* hybridization analysis of E9.5–E12.5 *Hoxb2*^{PolII} and *Hoxb4*^{PolII} mutant embryos. In each panel, genotypes of embryos are shown in the lower left and the probe used is shown in the upper right. (A–C) *Hoxb3* expression in hemisected E12.5 embryos. (A) E12.5 control embryo (*Hoxb4*$^{+/-}$), with strong *Hoxb3* expression in the ventral body wall (vb). (B) *Hoxb4*^{PolII} mutant embryo showing a similar *Hoxb3* staining pattern. (C) *Hoxb2*^{PolII} mutant embryo in which *Hoxb3* expression is strongly reduced or absent in the ventral body wall (vb). (D) *AP2* expression in a wild-type embryo at E9.5 (~24 somites). (E) *AP2* expression in a *Hoxb4*^{PolII} mutant embryo is similar to controls. (F) *Alx3* expression in an E11 whole-mount wild-type embryo. (G) *Alx3* expression appears similar in a *Hoxb4*^{PolII} mutant embryo. (H) In a transverse pattern section, *Alx3* staining can be seen in the ventral body wall (arrow) in controls. (I) In a *Hoxb4*^{PolII} mutant, *Alx3* expression in the ventral body wall is dramatically reduced (arrow). Note that the morphology of the body wall is similar to controls, and that staining in other areas (asterisk) remains strong. h, heart; to, tongue.

the sternal defects in the *Hoxb4*^{r} allele are likely caused by effects on neighboring *HoxB* genes.

In contrast, our *Hoxb4*^{PolII} phenotype is more severe than all other reported alleles of *Hoxb4*, with >90% penetrance of a general defect in ventral body wall formation, and a 40–50% incidence of embryonic lethality. While the neonatal lethality and ventral body wall phenotype of *Hoxb4*^{PolII} mutants is similar in many respects to that reported for the *HoxBΔ1* deletion, no embryonic lethality was observed for *HoxBΔ1* (Medina-Martinez *et al.*, 2000). As *Hoxb4*^{PolII} heterozygotes are normal, it is unlikely that this phenotypic difference is due to the *PolII-neo* cassette causing over- or misexpression of neighboring *HoxB* genes, or that aberrant transcripts initiating in the *neo* cassette contribute to the phenotype. This raises the interesting possibility that the increased severity of the *Hoxb4*^{PolII} allele relative to the *HoxBΔ1* deletion is due to an imbalance in *HoxB* gene expression, and that the phenotype is not due solely to loss of *Hoxb2* and *Hoxb4* function.

Differences in genetic background may also affect phenotypic severity. Ramirez-Solis *et al.* (1993) did report a difference in the penetrance of the sternal phenotype of *Hoxb4*^{r} with genetic background, with 129SvEv inbred mice having completely penetrant defects and neonatal death while the 129 × C57BL6 mice had lowered penetrance and 50% survival. Interestingly, phenotypes in both the *Hoxb4*^{PolII} and *Hoxb4*^{nl} alleles become more severe as mice were successively backcrossed onto a more inbred, C57BL6 background; the only two *Hoxb4*^{PolII} mutants without a fully split sternum were from early F_2 generation crosses. A similar effect could also contribute to the differences between the *HoxBΔ1* and *Hoxb4*^{PolII} phenotypes, since the *HoxBΔ1* analysis was performed using F_1 intercross progeny (Medina-Martinez *et al.*, 2000). Genetic background differences could also be involved in the differences in the severity and penetrance of the body wall defects seen in the *Hoxb4*^{PolII} and *Hoxb2*^{PolII} alleles.

Ventral Body Wall Defects May Involve Loss of Alx3 and Alx4

The interaction between *Hoxb2* and *Hoxb4* in ventral body wall formation appears to involve both r6 neural crest and ventral body wall structures (Barrow and Capecchi, 1996). This raises the possibility that defects in both neural crest cells and the ventral body wall itself are necessary to generate this phenotype. This result makes clear the difficulty in predicting the full range of functions of these genes based on overlap in expression patterns alone, as phenotypic interactions can also occur via a combination of defects in interacting tissues. Mutations in other genes expressed in either of these two cell types have been shown to cause ventral body wall defects, including *AP-2* (Zhang *et al.*, 1996) and members of the paired-type *aristaless* family of transcription factors (ten Berge *et al.*, 1998; Qu *et al.*, 1999). *AP-2* is expressed in all migrating neural crest, and *AP-2* mutants have profound defects in body wall formation (Zhang *et al.*, 1996). *AP-2* expression in the *Hoxb4*^{PolII} mutants was indistinguishable from controls. Therefore, the observed morphological defects do not appear to be due to defective NCC migration, although we cannot rule out a defect in the generation or migration of a subset of NCC. A more intriguing possibility is that the phenotypes may involve defects in NCC function due to the loss of *Hoxb2* expression in those cells (Barrow and Capecchi, 1996).

We used *Alx3* and *Alx4* as markers for the ventral body wall. *Alx3* and *Alx4* are members of the *aristaless* family of homeobox genes, which also includes *Cart-1* (Qu *et al.*, 1997; ten Berge *et al.*, 1998). *Alx3* and *Alx4* are both expressed in the ventral body wall at E10.5–E11.5, and *Alx4/Cart-1* double mutants have a split sternum phenotype (Qu *et al.*, 1999). In contrast to the results with *AP-2*, both *Alx3* and *Alx4* expression are down regulated in the ventral body wall of *Hoxb4*^{PolII} mutants, before the appearance of a morphological defect. The loss of expression is specific, as *Alx3/4* expression is normal at other locations, and *Hoxb3* is still expressed in the ventral body wall in *Hoxb4*^{PolII} mutants as late as E12.5. This result suggests a regulatory cascade in the ventral body wall, with *aristaless* genes acting downstream of *Hox* genes in the formation and closure of the ventral body wall.

The Hoxb4^{PolII} *Phenotype Is Similar to a Human Syndrome, Pentalogy of Cantrell*

The array of defects in the *Hoxb4*^{PolII} mutants is strikingly similar to a rare congenital disorder in humans, Pentalogy of Cantrell. This syndrome is characterized by sternal clefts, pericardial and diaphragmatic defects, midline supraumbilical abdominal wall defect, and cardiac abnormalities, and has an estimated frequency of about 5 per million live births (Cantrell *et al.*, 1958; Carmi and Boughman, 1992). Two studies have found evidence for a genetic contribution, one suggesting X-linkage (Martin *et al.*, 1992), and another autosomal gene involvement (Bird *et al.*, 1994). Since in our mouse model at least two genes are involved in generating this severe phenotype, it is perhaps not surprising that elucidating the genetic basis for this disorder in humans has proven difficult. Our results show a possible genetic mechanism for this disorder.

ACKNOWLEDGMENTS

We thank M. Allen, S. Barnett, C. Lenz, E. Nakashima, and G. Peterson at the University of Utah and S. Navarre at the Medical College of Georgia for excellent technical assistance. B. Headrick in the IMMAG Electron Microscopy/Histology Core Facility at the Medical College of Georgia supplied technical assistance with histology. J.R.B. was supported by an NIH Developmental Biology Training Grant (5T32 HD07491).

REFERENCES

Araki, K., Araki, M., Miyazaki, J. I., and Vassalli, P. (1995). Site-specific recombination of a transgene in fertilized eggs by transcient expression of Cre-recombinase. *Proc. Natl. Acad. Sci. USA* **92,** 160–164.

Barrow, J. R., and Capecchi, M. R. (1996). Targeted disruption of the *hoxb-2* locus in mice interferes with expression of *hoxb-1* and *hoxb-4*. *Development* **122,** 3817–3828.

Barrow, J. R., and Capecchi, M. R. (1999). Compensatory defects associated with mutations in *Hoxa1* restore normal palatogenesis to *Hoxa2* mutants. *Development* **126,** 5011–5026.

Bird, L. M., Newbury, R. O., Ruiz-Velasco, R., and Jones, M. C. (1994). Recurrence of diaphragmatic agenesis associated with multiple midline defects: Evidence for an autosomal gene regulating the midline [see comments]. *Am. J. Med. Genet.* **53,** 33–38.

Cantrell, J., Haller, J., and Ravitch, M. (1958). A syndrome of congenital defects involving the abdominal wall, sternum, diaphragm, pericardium, and heart. *Surg. Gynecol. Obstet.* **107,** 602–614.

Carmi, R., and Boughman, J. A. (1992). Pentalogy of Cantrell and associated midline anomalies: a possible ventral midline developmental field. *Am. J. Med. Genet.* **42,** 90–95.

Carpenter, E. M., Goddard, J. M., Chisaka, O., Manley, N. R., and Capecchi, M. R. (1993). Loss of *Hox-A1* (*Hox-1.6*) function results in the reorganization of the murine hindbrain. *Development* **118,** 1063–1075.

Chen, F., and Capecchi, M. R. (1997). Targeted mutations in *Hoxa-9* and *Hoxb-9* reveal synergistic interactions. *Dev. Biol.* **181,** 186–196.

Chen, F., and Capecchi, M. R. (1999). Paralogous mouse *Hox* genes, *Hoxa9*, *Hoxb9*, and *Hoxd9*, function together to control development of the mammary gland in response to pregnancy. *Proc. Natl. Acad. Sci. USA* **96,** 541–546.

Condie, B. G., and Capecchi, M. R. (1994). Mice with targeted disruptions in the paralogous genes *hoxa-3* and *hoxd-3* reveal synergistic interactions. *Nature* **370,** 304–307.

Davis, A. P., and Capecchi, M. R. (1996). A mutational analysis of the 5′ *Hox D* genes: Dissection of genetic interactions during limb development in the mouse. *Development* **122,** 1175–1185.

Davis, A. P., Witte, D. P., Hsieh-Li, H. M., Potter, S. S., and Capecchi, M. R. (1995). Absence of radius and ulna in mice lacking *hoxa-11* and *hoxd-11*. *Nature* **375,** 791–795.

Deng, C., Thomas, K. R., and Capecchi, M. R. (1993). Location of crossovers during gene targeting with insertion and replacement vectors. *Mol. Cell. Biol.* **13,** 2134–2140.

Favier, B., Rijli, F. M., Fromental-Ramain, C., Fraulob, V., Chambon, P., and Dollé, P. (1996). Functional cooperation between the non-paralogous genes *Hoxa-10* and *Hoxd-11* in the developing forelimb and axial skeleton. *Development* **122,** 449–460.

Fromental-Ramain, C., Warot, X., Lakkaraju, S., Favier, B., Haack, H., Birling, C., Dierich, A., Dollé, P., and Chambon, P. (1996a). Specific and redundant functions of the paralogous *Hoxa-9* and *Hoxd-9* genes in forelimb and axial skeleton patterning. *Development* **122,** 461–472.

Fromental-Ramain, C., Warot, X., Messadecq, N., LeMeur, M., Dollé, P., and Chambon, P. (1996b). *Hoxa-13* and *Hoxd-13* play a crucial role in the patterning of the limb autopod. *Development* **122,** 2997–3011.

Gavalas, A., Studer, M., Lumsden, A., Rijli, F. M., Krumlauf, R., and Chambon, P. (1998). *Hoxa1* and *Hoxb1* synergize in patterning the hindbrain, cranial nerves and second pharyngeal arch. *Development* **125,** 1123–1136.

Goddard, J. M., Rossel, M., Manley, N. R., and Capecchi, M. R. (1996). Mice with targeted disruption of *Hoxb-1* fail to form the motor nucleus of the VIIth nerve. *Development* **122,** 3217–3228.

Graham, A., Papalopulu, N., Lorimer, J., McVey, J. H., Tuddenham, E. G., and Krumlauf, R. (1988). Characterization of a murine homeo box gene, *Hox-2.6*, related to the Drosophila Deformed gene. *Genes Dev.* **2,** 1424–1438.

Horan, G. S. B., Kovàcs, E. N., Behringer, R. R., and Featherstone, M. S. (1995a). Mutations in paralogous *Hox* genes result in overlapping homeotic transformations of the axial skeleton: Evidence for unique and redundant function. *Dev. Biol.* **169,** 359–372.

Horan, G. S. B., Ramírez-Solis, R., Featherstone, M. S., Wolgemuth, D. J., Bradley, A., and Behringer, R. R. (1995b). Compound mutants for the paralogous *hoxa-4*, *hoxb-4*, and *hoxd-4* genes show more complete homeotic transformations and a dose-dependent increase in the number of vertebrae transformed. *Genes Dev.* **9,** 1667–1677.

Manley, N. R., and Capecchi, M. R. (1995). The role of *hoxa-3* in mouse thymus and thyroid development. *Development* **121,** 1989–2003.

Manley, N. R., and Capecchi, M. R. (1997). *Hox* group 3 paralogous genes act synergistically in the formation of somitic and neural crest-derived structures. *Dev. Biol.* **192,** 274–288.

Manley, N. R., and Capecchi, M. R. (1998). *Hox* group 3 paralogs regulate the development and migration of the thymus, thyroid and parathyroid glands. *Dev. Biol.* **195,** 1–15.

Mansour, S. L., Thomas, K. R., and Capecchi, M. R. (1988). Disruption of the proto-oncogene *int-2* in mouse embryo-derived stem cells: A general strategy for targeting mutations to non-selectable genes. *Nature* **336,** 348–352.

Martin, R., Cunniff, C., Erickson, L., and Jones, K. (1992). Pentalogy of Cantrell and ectopia cordis, a familial developmental field complex. *Am. J. Med. Genet.* **42,** 839–841.

Medina-Martinez, O., Bradley, A., and Ramírez-Solis, R. (2000). A large targeted deletion of *Hoxb1–Hoxb9* produces a series of single-segment anterior homeotic transformations. *Dev. Biol.* **222,** 71–83.

Qu, S., Li, L., and Wisdom, R. (1997). Alx-4: cDNA cloning and characterization of a novel paired-type homeodomain protein. *Gene* **203,** 217–223.

Qu, S., Tucker, S. C., Zhao, Q., deCrombrugghe, B., and Wisdom, R. (1999). Physical and genetic interactions between Alx4 and Cart1. *Development* **126,** 359–369.

Ramírez-Solis, R., Zheng, H., Whiting, J., Krumlauf, R., and Bradley, A. (1993). *Hoxb-4* (*Hox-2.6*) mutant mice show homeotic transformation of a cervical vertebra and defects in the closure of the sternal rudiments. *Cell* **73,** 279–294.

Rancourt, D. E., Tsuzuki, T., and Capecchi, M. R. (1995). Genetic interaction between *hoxb-5* and *hoxb-6* is revealed by nonallelic noncomplementation. *Genes Dev.* **9,** 108–122.

Rossel, M., and Capecchi, M. R. (1999). Mice mutant for both *Hoxa1* and *Hoxb1* show extensive remodeling of the hindbrain and defects in craniofacial development. *Development* **126,** 5027–5040.

Studer, M., Gavalas, A., Marshall, H., Ariza-McNaughton, L., Rijli, F. M., Chambon, P., and Krumlauf, R. (1998). Genetic interactions between *Hoxa1* and *Hoxb1* reveal new roles in regulation of early hindbrain patterning. *Development* **125,** 1025–1036.

ten Berge, D., Brouwer, A., el Bahi, S., Guenet, J. L., Robert, B., and Meijlink, F. (1998). Mouse Alx3: an aristaless-like homeobox gene expressed during embryogenesis in ectomesenchyme and lateral plate mesoderm. *Dev. Biol.* **199,** 11–25.

Zákány, J., and Duboule, D. (1996). Synpolydactyly in mice with a targeted deficiency in the *HoxD* complex. *Nature* **384,** 69–71.

Zhang, J., Hagopian-Donaldson, S., Serbedzija, G., Elsemore, J., Plehn-Dujowich, D., McMahon, A. P., Flavell, R. A., and Williams, T. (1996). Neural tube, skeletal and body wall defects in mice lacking transcription factor AP-2. *Nature* **381,** 238–241.

Received for publication May 3, 2001
Revised June 11, 2001
Accepted June 14, 2001
Published online July 31, 2001